

\mathcal{L}_1 Adaptive Controller for a Missile Longitudinal Autopilot Design

Jiang Wang *

Virginia Tech, Blacksburg, VA 24061, USA

Chengyu Cao †

University of Connecticut, Storrs, CT, 06269, USA

Naira Hovakimyan ‡

University of Illinois at Urbana-Champaign, Urbana, IL 61801, USA

Richard E. Hindman § and D. Brett Ridgely ¶

Raytheon Missile Systems, Tucson, AZ 85734, USA

This paper considers application of \mathcal{L}_1 adaptive output feedback controller to a missile longitudinal autopilot design. The proposed adaptive controller has satisfactory performance in the presence of parametric uncertainties and time-varying disturbances. Simulations demonstrate the benefits of the control method and compare the results to Linear Quadratic Regulator (LQR) and Linear Quadratic Gaussian (LQG) with Loop Transfer Recovery (LTR) design.

I. Introduction

This paper presents the application of an \mathcal{L}_1 adaptive output feedback controller to longitudinal autopilot design for a missile in the presence of uncertainties in system dynamics. The uncertainties include parametric variations in the transfer function and time-varying disturbances. The parametric variations of the system's transfer function are caused by changes in aerodynamic coefficients. The missile model, taken from Mracek and Ridgely [1], is an unstable non-minimum phase system. The nominal optimal controller in Mracek and Ridgely [1] uses both system outputs (pitch rate and normal acceleration) to compute the feedback control signal. In this paper we only use the acceleration.

The proposed adaptive output feedback controller, taken from Cao and Hovakimyan [2, 3], allows tracking of reference systems that do not verify the SPR condition for their input-output transfer functions. Similar to the earlier

*Graduate Research Assistant, Student Member AIAA, Department of Aerospace and Ocean Engineering, 215 Randolph Hall; jwang005@vt.edu (Corresponding Author).

†Research Assistant Professor, Member AIAA, Department of Mechanical Engineering; ccao@enr.uconn.edu

‡Professor, Associate Fellow AIAA, Department of Mechanical Science and Engineering; nhovakim@illinois.edu

§Principal Systems Engineer, Member AIAA, Rick.Hindman@raytheon.com

¶Senior Department Manager, Senior Member AIAA, dbridgely@raytheon.com

results of Cao and Hovakimyan [4], the \mathcal{L}_∞ -norms of both input/output error signals between the closed-loop adaptive system and the reference system can be rendered arbitrarily small by reducing the step-size of integration. The key difference between [2,3] and [4] is the new piece-wise continuous adaptive law which enables tracking of the reference systems without imposing the SPR requirement on their input-output transfer function. The adaptive control is defined as the output of a low-pass filter, resulting in a continuous signal despite the discontinuity of the adaptive law. The \mathcal{L}_1 adaptive output feedback controller aims at achieving a guaranteed transient performance for the system's output, and regulating the frequency spectrum and the performance bound for the system's input signal as well, by rendering them arbitrarily close to the corresponding output/input signals of a bounded reference system.

We consider the longitudinal dynamics of a missile in the presence of uncertainties in aerodynamics and time-varying disturbances. For comparison purposes, we first consider the nominal optimal controller from Mracek and Ridgely [1], which is a "classic" three-loop topology autopilot designed by LQR methods. Then assuming only measured acceleration is available, we design a LQG controller with Loop Transfer Recovery (LTR) to recover the robustness of the LQR controller. This serves as the nominal output feedback controller in the absence of uncertainties. We augment the baseline LQG controller by \mathcal{L}_1 adaptive output feedback loop to compensate for the modeling uncertainties.

The paper is organized as follows. Section II presents the problem formulation. Section III shows the nominal controller design. Section IV gives an overview of the key results from Cao and Hovakimyan [2, 3], and Section V discusses some design solutions to achieve the desired performance specifications. Section VI presents the simulations, while Section VII concludes the paper.

II. Problem Formulation

The missile's longitudinal dynamics can be described using the short period approximation of the longitudinal equations of motion [1]:

$$\dot{x}_p(t) = A_p x_p(t) + B_p [\delta_p(t) + v(t, y(t))] \quad (1)$$

$$y_p(t) = C_p x_p(t) + D_p [\delta_p(t) + v(t, y(t))] \quad (2)$$

$$y(t) = A_{z_m}(t), \quad (3)$$

where $\delta_p(t)$ is the elevator input, $v(t, y(t))$ is time-varying disturbance and depends on $y(t)$, $x_p(t)$ and $y_p(t)$ are the state and the output vectors respectively, given by

$$x_p(t) = \begin{bmatrix} \alpha(t) \\ q(t) \end{bmatrix}, \quad y_p(t) = \begin{bmatrix} A_{z_m}(t) \\ q_m(t) \end{bmatrix}, \quad (4)$$

while $\alpha(t)$ is angle of attack, $q(t)$ is pitch rate, $A_{z_m}(t)$ is normal acceleration and $q_m(t)$ is measured pitch rate. In (1) and (2) the system matrices are

$$A_p = \begin{bmatrix} \frac{1}{V_{m_0}} \left[\frac{\bar{Q} S C_{z_{\alpha 0}}}{m} - A_{X_0} \right] & 1 \\ \frac{\bar{Q} S d C_{m_{\alpha 0}}}{I_{YY}} & 0 \end{bmatrix}, \quad B_p = \begin{bmatrix} \frac{\bar{Q} S C_{z_{\delta p_0}}}{m V_{m_0}} \\ \frac{\bar{Q} S d C_{m_{\delta p_0}}}{I_{YY}} \end{bmatrix},$$

$$C_p = \begin{bmatrix} \frac{\bar{Q} S C_{z_{\alpha 0}}}{m g} - \frac{\bar{Q} S d C_{m_{\alpha 0}} \bar{x}}{g I_{YY}} & 0 \\ 0 & 1 \end{bmatrix}, \quad D_p = \begin{bmatrix} \frac{\bar{Q} S C_{z_{\delta p_0}}}{m g} - \frac{\bar{Q} S d C_{m_{\delta p_0}} \bar{x}}{g I_{YY}} \\ 0 \end{bmatrix}.$$

The numerical values of the simulation example in this paper are listed in Table 1, and are taken from Mracek and Ridgely [1]. In this paper we consider uncertainties in the aerodynamic coefficients $C_{z_{\alpha 0}}$, $C_{m_{\alpha 0}}$, $C_{z_{\delta p_0}}$ and $C_{m_{\delta p_0}}$.

Table 1. Numerical Values of Model

Variable	Value	Units	Description
V_{m_0}	3350	ft/sec	Total Missile Velocity
m	11.1	slug	Total Missile Mass
I_{YY}	137.8	slug – ft ²	Pitch Moment of Inertia
\bar{x}	1.2	ft	Distance from CG to IMU Positive Forward
A_{X_0}	-60	ft/sec ²	Axial Acceleration Positive Forward
$C_{z_{\alpha 0}}$	-5.5313	-	Pitch Force Coefficient due to Angle of Attack
$C_{m_{\alpha 0}}$	6.6013	-	Pitch Moment Coefficient due to Angle of Attack
$C_{z_{\delta p_0}}$	-1.2713	-	Pitch Force Coefficient due to fin Deflection
$C_{m_{\delta p_0}}$	-7.5368	-	Pitch Moment Coefficient due to fin Deflection
\bar{Q}	13332	lb/ft ²	Dynamic Pressure
S	0.5454	ft ²	Reference Area
d	0.8333	ft	Reference Length
g	32.174	ft/sec ²	Gravity Constant

These uncertainties do not satisfy the restrictive “matching condition” required by conventional adaptive feedback control schemes. Therefore we apply the adaptive output feedback method from Cao and Hovakimyan [2,3].

We assume that the maximum possible variations of aerodynamic coefficients with respect to nominal values are known conservatively:

$$\|\Delta C_{z_{\alpha 0}}\| \leq 0.5 \cdot \|C_{z_{\alpha 0}}\|, \quad \|\Delta C_{m_{\alpha 0}}\| \leq 0.5 \cdot \|C_{m_{\alpha 0}}\|,$$

$$\|\Delta C_{z_{\delta p_0}}\| \leq 0.5 \cdot \|C_{z_{\delta p_0}}\|, \quad \|\Delta C_{m_{\delta p_0}}\| \leq 0.5 \cdot \|C_{m_{\delta p_0}}\|,$$

while the exact values of these coefficients are unknown. In simulations, the actual values of aerodynamic coefficients

are selected to be

$$C'_{z_{\alpha_0}} = 1.4 \cdot C_{z_{\alpha_0}}, \quad C'_{m_{\alpha_0}} = 1.4 \cdot C_{m_{\alpha_0}}, \quad C'_{z_{\delta_{p_0}}} = 0.7 \cdot C_{z_{\delta_{p_0}}}, \quad C'_{m_{\delta_{p_0}}} = 0.7 \cdot C_{m_{\delta_{p_0}}}. \quad (5)$$

The control objective is to design adaptive output feedback controller to achieve satisfactory tracking performance for the output $A_{z_m}(t)$, in the presence of parametric uncertainties and time-varying disturbances, using only $A_{z_m}(t)$.

III. Nominal Controller Design

III.A. LQR solution

We first develop the ‘‘classical’’ three-loop topology for the nominal controller design [1], assuming that the required output signals in the three-loop topology are available. The system is augmented by considering $z(t) = \delta_p(t) + v(t, y(t))$ as an additional state:

$$\begin{aligned} \dot{x}_1(t) &= A_1 x_1(t) + B_1 (u(t) + d(t, y(t))) \\ y_1(t) &= C_1 x_1(t), \end{aligned} \quad (6)$$

where

$$x_1(t) = \begin{bmatrix} \alpha(t) \\ q(t) \\ z(t) \end{bmatrix}, \quad u(t) = \dot{\delta}_p(t), \quad d(t, y(t)) = \dot{v}(t, y(t)), \quad y_1(t) = \begin{bmatrix} A_{z_m}(t) \\ q_m(t) \\ \dot{q}_m(t) \end{bmatrix}, \quad (7)$$

and the transformed state space matrices are

$$A_1 = \begin{bmatrix} A_p & B_p \\ [0] & 0 \end{bmatrix}, \quad B_1 = \begin{bmatrix} [0] \\ 1 \end{bmatrix}, \quad C_1 = \begin{bmatrix} C_p & D_p \\ A_p(2, :) & B_p(2, :) \end{bmatrix}. \quad (8)$$

We also assume that the time-varying disturbance $d(t, y(t))$ satisfies the following assumption.

Assumption 1 *There exists a constant $L > 0$ such that the following inequality holds uniformly in $t \geq 0$ for all y, y' :*

$$|d(t, y) - d(t, y')| \leq L|y - y'|$$

A block diagram of the plant and controller structure is shown in Fig. 1.

When the aerodynamic uncertainties in (5) and the disturbance $d(t, y(t))$ are not present, the optimal Linear Quadratic Regulator (LQR) solution in [1] is given by:

$$u(t) = \dot{\delta}_p(t) = K_{opt} \begin{bmatrix} A_{z_m}(t) - K_{ss} r_0 \\ q_m(t) \\ \dot{q}_m(t) \end{bmatrix}, \quad (9)$$

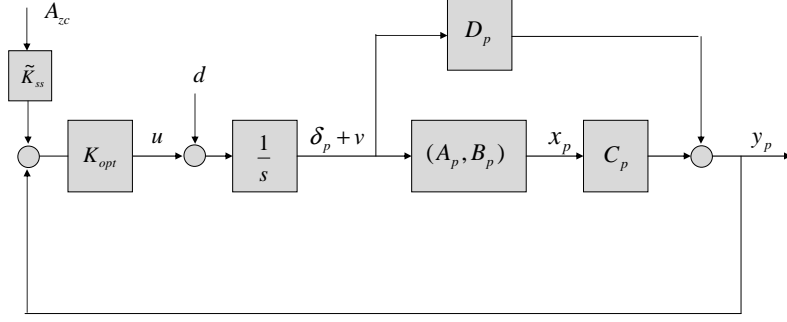


Figure 1. Block diagram of system.

where K_{ss} is chosen to ensure zero steady-state error for step commands, while r_0 is the steady-state value of the reference command $r(t)$. Based on the nominal numerical values given in Table 1, the optimal controller gains are:

$$K_{opt} = [-1.3028 \quad 11.7544 \quad 0.3277], \quad K_{ss} = 1.0855.$$

In the current setup, $\dot{q}_m(t)$ is not measurable, and the above computed optimal controller is actually the derivative of $\delta_p(t)$. Since we have a linear system, we can integrate both sides of (9) to determine $\delta_p(t)$ (assuming constant gains) as:

$$\delta_p(t) = K_{opt} \begin{bmatrix} \int_0^t (A_{z_m}(\tau) - K_{ss}r_0) d\tau \\ \int_0^t q_m(\tau) d\tau \\ \int_0^t \dot{q}_m(\tau) d\tau \end{bmatrix} = K_{opt} \begin{bmatrix} \int_0^t (A_{z_m}(\tau) - K_{ss}r_0) d\tau \\ \int_0^t q_m(\tau) d\tau \\ q_m(t) \end{bmatrix}. \quad (10)$$

If the available feedback signal is only A_{z_m} , the above optimal controller cannot be implemented. The proposed adaptive control method can have satisfactory tracking performance in the presence of parametric uncertainties and disturbance, using only A_{z_m} as feedback signal. For comparison purposes, we design an observer that can recover the original LQR control performance. At the same time we need to recover the inherent robustness of baseline LQR controller as much as possible, because we are looking into the controller's robustness to parametric uncertainties and disturbance.

III.B. Output feedback solution: LQG/LTR

Based on the LQR solution of the above nominal optimal control, we can design a Linear Quadratic Gaussian (LQG) with Loop Transfer Recovery (LTR) controller using only the output A_{z_m} . Since the LQR controller is ready, we only need to design the Kalman filter which can help recover the robustness of LQR controller. We note that due to the non-minimum phase property of the system, the robustness recovery is limited.

In Mracek and Ridgely [1], the LQR design is based on the transformed system with state transformation $x_2 = C_1x_1$, as shown below

$$\begin{aligned} \dot{x}_2(t) &= A_2x_2(t) + B_2u(t) \\ y_2(t) &= x_2(t) \end{aligned} \quad (11)$$

where

$$x_2(t) = \begin{bmatrix} A_{z_m}(t) \\ q_m(t) \\ \dot{q}_m(t) \end{bmatrix}, \quad A_2 = C_1 A_1 C_1^{-1}, \quad B_2 = C_1 B_1.$$

We design a Kalman filter based on this LQR solution. Plant noise and measurement noise are introduced to produce

$$\begin{aligned} \dot{x}_2(t) &= A_2 x_2(t) + B_2 u(t) + B_2 \omega(t) \\ y_k(t) &= A_{z_m}(t) x_2(t) + v(t) \end{aligned} \quad (12)$$

where the plant noise $\omega(t)$ and the measurement noise $v(t)$ are white noises with the spectral densities S_ω and S_v respectively, and they are uncorrelated and orthogonal. Furthermore, the plant noise and the initial states of the system (12) are assumed to be uncorrelated and orthogonal; so are the measurement noise and the states. The Kalman filter equation is

$$\dot{\hat{x}}_2(t) = A_2 \hat{x}_2(t) + B_2 u(t) + G(y_k(t) - [1 \ 0 \ 0] \hat{x}_2(t)) \quad (13)$$

where G is the Kalman gain. The Loop Transfer Recovery design is done by increasing the spectral density S_ω of the plant noise $\omega(t)$. We choose different values of S_ω to design the Kalman filter, and compare the results to the LQR results. The spectral density of the measurement noise is set as $S_v = 0.1$. The Kalman filter gain is obtained by MATLAB command “*kalman*”. Next we show the system response of LQG/LTR control.

First, the unit step responses of the LQR and LQG/LTR control are shown. In Fig. 2, the LQG controller is designed with $S_\omega = 1$ and $S_v = 0.1$. It can be seen that the time responses of these two controllers are identical. However, the robustness of these two controllers are different, due to the small value of spectral density S_ω , which means that the loop transfer recovery is not enough. This can be seen in Fig. 3. In this figure, the parametric uncertainties in (5) are present. The LQR controller has certain inherent robustness to parametric uncertainties, hence its performance is acceptable. However, the LQG controller has degraded performance due to lack of robustness. We need to increase the spectral density S_ω to recover as much as possible the robustness of the LQR controller. In Fig. 4, the spectral density is increased to 100, and we can see that the performance is improved in the presence of parametric uncertainties. This robustness recovery is limited by the system’s non-minimum phase property. Hence, increasing S_ω cannot recover the robustness completely, as shown in Fig. 5. With very large value of S_ω , the system’s performance is no better than that in the case of smaller S_ω .

We now introduce a disturbance $d(t) = 0.1 \sin(0.5\pi t)$ into the system. In Fig. 6, the system output under the LQR controller drifts from the desired steady state position, and the performance of LQG/LTR is also unacceptable. This is expected because of the limitation of the loop transfer recovery applied to a non-minimum phase system.

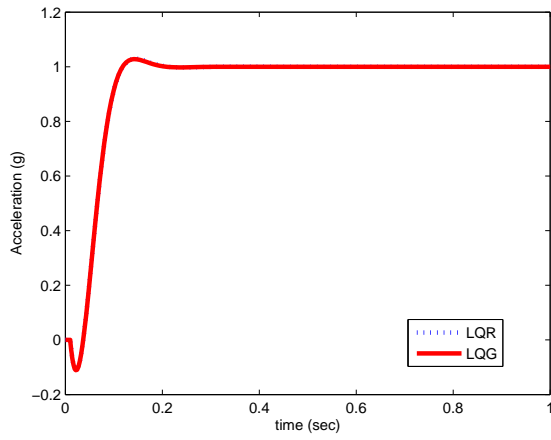


Figure 2. Comparison between LQR and LQG - no uncertainty, no disturbance

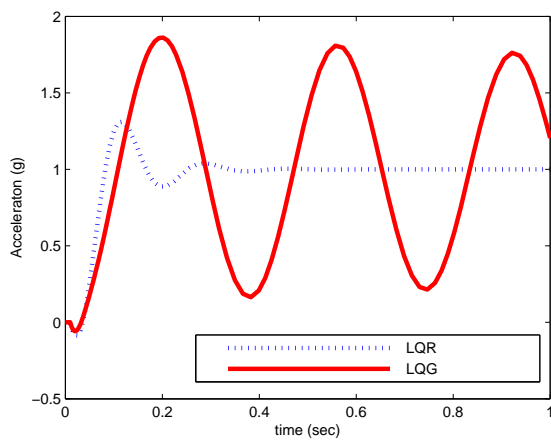


Figure 3. Comparison between LQR and LQG - with uncertainty, no disturbance

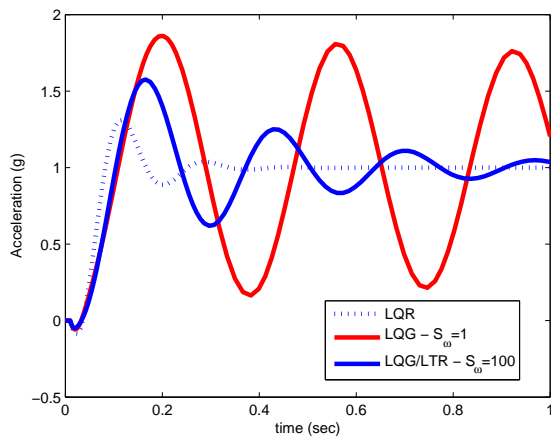


Figure 4. Comparison between LQR, LQG and LQG/LTR - with uncertainty, no disturbance

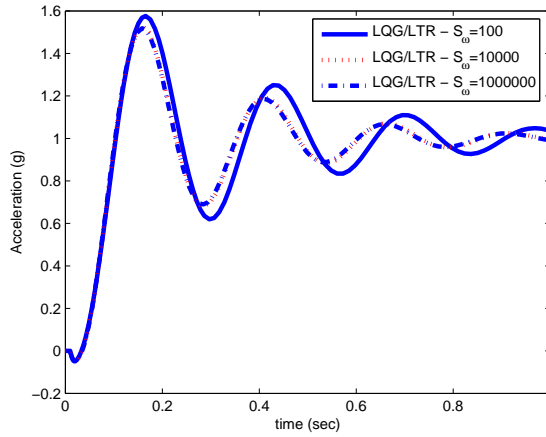


Figure 5. Different values of S_ω for LQG/LTR designs - with uncertainties, no disturbance

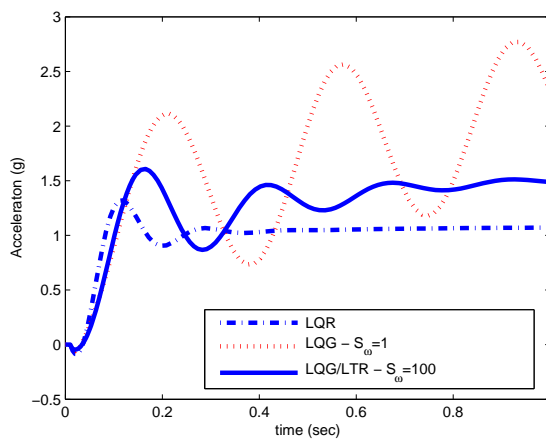


Figure 6. Comparison between LQR, LQG and LQG/LTR - with uncertainties and disturbance

IV. \mathcal{L}_1 Adaptive Output Feedback Control

In system (6), if we let $y(t) = C_1(1, :)x_1(t) = c^\top x_1(t) = A_{z_m}(t)$, the longitudinal dynamics of the missile can be presented in the following form:

$$y(s) = A(s) [u(s) + d(s)] , \quad y(0) = 0 , \quad (14)$$

where $u(t) = \dot{\delta}_p(t) \in \mathbb{R}$ is the input, $y(t) = A_{z_m}(t) \in \mathbb{R}$ is the system output, $A(s) = c^\top (s\mathbb{I} - A_1)^{-1} B_1$ is the unknown transfer function of the system, $d(s)$ is the Laplace transform of the time-varying disturbances in (6). Notice that $d(t, y)$ depends on the system output y , and the upper bound of the growth rate of $d(t, y)$ with respect to y is L , as stated in Assumption 1.

Substituting the numerical values from Table 1 into the system in (6), we get the nominal system of $A(s)$

$$A_0(s) = \frac{A_{0n}}{A_{0d}} = \frac{-13.51s^2 + 16.46s + 44800}{s^3 + 1.064s^2 - 290.3s} . \quad (15)$$

To achieve the control objective, we need to design an adaptive output feedback controller $u(t)$ such that in the presence of uncertainties the system output $y(t)$ tracks the reference input $r(t)$ with satisfactory performance. This can be done by selecting a minimum-phase, strictly proper and stable transfer function $M(s)$, and designing an adaptive control law to achieve $y(s) \approx M(s)r(s)$. The selection of $M(s)$ needs to satisfy the sufficient conditions for stability and performance, and we postpone the discussion on selection of $M(s)$ to Section V. The system in (14) can be rewritten as:

$$y(s) = M(s) (u(s) + \sigma(s)) \quad (16)$$

$$\sigma(s) = \left((A(s) - M(s))u(s) + A(s)d(s) \right) / M(s) . \quad (17)$$

Let $(A_m \in \mathbb{R}^{N \times N}, b_m \in \mathbb{R}^N, c_m \in \mathbb{R}^N)$ be the minimal realization of $M(s)$. Hence, (A_m, b_m, c_m) is controllable and observable, with A_m being Hurwitz. Thus, the system in (16) can be rewritten as:

$$\dot{x}(t) = A_m x(t) + b_m (u(t) + \sigma(t)) \quad (18)$$

$$y(t) = c_m^\top x(t), \quad x(0) = x_0 = 0.$$

Next we introduce the closed-loop *reference system* that defines an *achievable control objective* for the \mathcal{L}_1 adaptive controller.

Closed-loop reference system: The reference system is given by

$$y_{ref}(s) = M(s)(u_{ref}(s) + \sigma_{ref}(s)) \quad (19)$$

$$\sigma_{ref}(s) = \left((A(s) - M(s))u_{ref}(s) + A(s)d_{ref}(s) \right) / M(s)$$

$$u_{ref}(s) = C(s)(r(s) - \sigma_{ref}(s))$$

where $C(s)$ is a low pass filter with DC gain $C(0) = 1$.

According to [2, Lemma 1] the selection of $C(s)$ and $M(s)$ must ensure that

$$H(s) = A(s)M(s) / \left(C(s)A(s) + (1 - C(s))M(s) \right) \quad (20)$$

is stable and that the \mathcal{L}_1 -gain of the cascaded system is upper bounded as follows:

$$\|H(s)(1 - C(s))\|_{\mathcal{L}_1} L < 1 \quad (21)$$

Then the reference system in (19) is stable.

The elements of the \mathcal{L}_1 adaptive controller are introduced next.

State predictor (passive identifier): Let $(A_m \in \mathbb{R}^{n \times n}, b_m \in \mathbb{R}^n, c_m \in \mathbb{R}^n)$ be the minimal realization of $M(s)$. Hence, (A_m, b_m, c_m) is controllable and observable with A_m being Hurwitz. Then the system in (14) can be rewritten as

$$\begin{aligned} \dot{x}(t) &= A_m x(t) + b_m(u(t) + \sigma(t)) \\ y(t) &= c_m^\top x(t) \end{aligned} \quad (22)$$

The state predictor is given by:

$$\begin{aligned} \dot{\hat{x}}(t) &= A_m \hat{x}(t) + b_m u(t) + \hat{\sigma}(t) \\ \hat{y}(t) &= c_m^\top \hat{x}(t) \end{aligned} \quad (23)$$

where $\hat{\sigma}(t) \in \mathbb{R}^n$ is the vector of adaptive parameters. Notice that in the state predictor equations $\hat{\sigma}(t)$ is not in the span of b_m , while in the equation (22) $\sigma(t)$ is in the span of b_m . Further, let $\tilde{y}(t) = \hat{y}(t) - y(t)$.

Adaptation law: Let P be the solution of the following algebraic Lyapunov equation:

$$A_m^\top P + P A_m = -Q$$

where $Q > 0$. From the properties of P it follows that there always exists a nonsingular \sqrt{P} such that

$$P = \sqrt{P}^\top \sqrt{P}.$$

Given the vector $c_m^\top (\sqrt{P})^{-1}$, let D be the $(n-1) \times n$ -dimensional nullspace of $c_m^\top (\sqrt{P})^{-1}$, i.e.

$$D(c_m^\top (\sqrt{P})^{-1})^\top = 0 \quad (24)$$

and let

$$\Lambda = \begin{bmatrix} c_m^\top \\ D\sqrt{P} \end{bmatrix} \in \mathbb{R}^{n \times n} \quad (25)$$

The update law for $\hat{\sigma}(t)$ is defined via the sampling time $T > 0^a$:

$$\hat{\sigma}(iT) = -\Phi^{-1}(T)\mu(iT), \quad i = 1, 2, \dots, \quad (26)$$

^a T defines the sampling rate of the available CPU.

where

$$\Phi(T) = \int_0^T e^{\Lambda A_m \Lambda^{-1}(T-\tau)} \Lambda d\tau \quad (27)$$

and

$$\mu(iT) = e^{\Lambda A_m \Lambda^{-1} T} \mathbf{1}_1 \tilde{y}(iT), \quad i = 1, 2, \dots \quad (28)$$

Here $\mathbf{1}_1$ denotes the basis vector in the space \mathbb{R}^n with its first element equal to 1 and other elements being zero.

Control law: The control law is defined via the output of the low-pass filter:

$$u(s) = C(s)r(s) - \frac{C(s)}{M(s)} c_m^\top (s\mathbb{I} - A_m)^{-1} \hat{\sigma}(s). \quad (29)$$

The complete \mathcal{L}_1 adaptive controller consists of the state predictor in (23), the adaptation law in (26), and the control law in (29), subject to the \mathcal{L}_1 -gain upper bound in (21). The performance bounds of the \mathcal{L}_1 adaptive output feedback controller are given by the following theorem.

Theorem 1

$$\begin{aligned} \lim_{T \rightarrow 0} (\|\tilde{y}\|_{\mathcal{L}_\infty}) &= 0 \\ \lim_{T \rightarrow 0} (\|y - y_{ref}\|_{\mathcal{L}_\infty}) &= 0 \\ \lim_{T \rightarrow 0} (\|u - u_{ref}\|_{\mathcal{L}_\infty}) &= 0 \end{aligned}$$

The result in this theorem follows immediately from [2, Theorem 1] and [2, Lemma 3].

V. Design Issues of \mathcal{L}_1 Adaptive Output Feedback Control

V.A. Stability

The first step of designing an \mathcal{L}_1 adaptive output feedback controller is to guarantee stability of the closed-loop system. From Theorem 1 it can be seen that the output of the closed-loop system tracks that of the closed-loop reference system arbitrarily closely for all $t > 0$. Hence the goal of the first step in the design is to find $C(s)$ and $M(s)$ to satisfy the sufficient conditions given in (20) and (21). These two conditions can guarantee the stability of closed-loop reference system.

We first discuss the classes of systems that can satisfy (20) via the choice of $M(s)$ and $C(s)$. We demonstrate that stability of $H(s)$ is equivalent to stabilization of $A(s)$ by

$$\frac{C(s)}{M(s)(1 - C(s))}. \quad (30)$$

Consider the closed-loop system, comprised of the system $A(s)$ and negative feedback of (30). The closed-loop transfer function is:

$$\frac{A(s)}{1 + A(s) \frac{C(s)}{M(s)(1 - C(s))}}. \quad (31)$$

Letting

$$A(s) = \frac{A_n(s)}{A_d(s)}, \quad C(s) = \frac{C_n(s)}{C_d(s)}, \quad M(s) = \frac{M_n(s)}{M_d(s)}, \quad (32)$$

it follows from (20) that

$$H(s) = \frac{C_d(s)M_n(s)A_n(s)}{H_d(s)}, \quad (33)$$

where

$$H_d(s) = C_n(s)A_n(s)M_d(s) + M_n(s)A_d(s)(C_d(s) - C_n(s)). \quad (34)$$

Incorporating (32), one can verify that the denominator of the system in (31) is exactly $H_d(s)$. Hence, stability of $H(s)$ is equivalent to the stability of the closed-loop system in (31).

The selection of $M(s)$ and $C(s)$ can be restricted due to the properties of the plant $A(s)$. Thus, it is not a trivial task. However, it can be done using linear systems theory. The essential objective in this step is to design, based on the nominal system $A_0(s)$, a feedback controller that can be decomposed into $C(s)$ and $M(s)$ according to the equation (30), while achieving stability of $H(s)$ in (20) and verifying the condition in (21) based on conservative knowledge of parametric variations in $A(s)$. In the following subsection we describe one method towards the selection of $C(s)$ and $M(s)$.

VA.1. Design via pole placement

We use a pole placement method (see examples in Ioannou and Sun [5]) to design a dynamic compensator for $A_0(s)$. The block diagram in Fig. 7 shows the structure of the closed-loop system, where the dynamic controller $P(s)/L(s)$ is determined by the solution of the following equation

$$A_{0_n}(s)P(s) + A_{0_d}(s)L(s) = A_{cl}(s). \quad (35)$$

All terms in (35) are polynomials of s . The Hurwitz polynomial $A_{cl}(s)$ defines the desired pole locations of the closed-loop system. The coefficients of polynomials $P(s)$ and $L(s)$ may be obtained by solving the algebraic equation

$$\beta_l = S_l^{-1}\alpha_l$$

containing the Sylvester matrix S_l of A_{0_n} and A_{0_d} , while β_l is a vector containing coefficients of both $P(s)$ and $L(s)$, and α_l is a vector containing coefficients of $A_{cl}(s)$ (defined next).

Definition 1 Given two polynomials $a(s) = a_n s^n + a_{n-1} s^{n-1} + \dots + a_0$, $b(s) = b_n s^n + b_{n-1} s^{n-1} + \dots + b_0$, the

Sylvester Matrix S_l is defined to be the following $2n \times 2n$ matrix:

$$S_l = \begin{bmatrix} a_n & 0 & 0 & \cdots & 0 & 0 & b_n & 0 & 0 & \cdots & 0 & 0 \\ a_{n-1} & a_n & 0 & & 0 & 0 & b_{n-1} & b_n & 0 & & 0 & 0 \\ \cdot & a_{n-1} & a_n & \ddots & & \vdots & \cdot & b_{n-1} & b_n & \ddots & & \vdots \\ \cdot & \cdot & \cdot & \cdot & \ddots & \vdots & \cdot & \cdot & \cdot & \cdot & \ddots & \vdots \\ \cdot & \cdot & \cdot & \cdot & \cdot & 0 & \cdot & \cdot & \cdot & \cdot & \cdot & 0 \\ a_1 & \cdot & \cdot & \cdot & \cdot & a_n & b_1 & \cdot & \cdot & \cdot & \cdot & b_n \\ a_0 & a_1 & \cdot & \cdot & \cdot & a_{n-1} & b_0 & b_1 & \cdot & \cdot & \cdot & b_{n-1} \\ 0 & a_0 & \cdot & \cdot & \cdot & \cdot & 0 & b_0 & \cdot & \cdot & \cdot & \cdot \\ 0 & 0 & \cdot & \cdot & \cdot & \cdot & 0 & 0 & \cdot & \cdot & \cdot & \cdot \\ \vdots & & \ddots & \cdot & \cdot & \cdot & \vdots & 0 & \ddots & \cdot & \cdot & \cdot \\ \vdots & & & \ddots & a_0 & a_1 & \vdots & & & \ddots & b_0 & b_1 \\ 0 & 0 & \cdots & 0 & 0 & a_0 & 0 & 0 & \cdots & 0 & 0 & b_0 \end{bmatrix}$$

Definition 2 If $L(s) = s^{n-1} + l_{n-2}s^{n-2} + \cdots + l_1s + l_0$, $P(s) = p_{n-1}s^{n-1} + p_{n-2}s^{n-2} + \cdots + p_1s + p_0$, then

$$\beta_l = [1, l_{n-2}, l_{n-3}, \cdots, l_1, l_0, p_{n-1}, p_{n-2}, \cdots, p_1, p_0]^\top.$$

If $A_{cl}(s) = s^{2n-1} + a_{2n-2}^*s^{2n-2} + \cdots + a_1^*s + a_0^*$, then

$$\alpha_l = [1, a_{2n-2}^*, a_{2n-3}^*, \cdots, a_1^*, a_0^*]^\top.$$

The polynomials $A_{0_n}(s)$ and $A_{0_d}(s)$ should be coprime to ensure the existence and uniqueness of solutions of $P(s)$ and $L(s)$, and non-singularity of S_l .

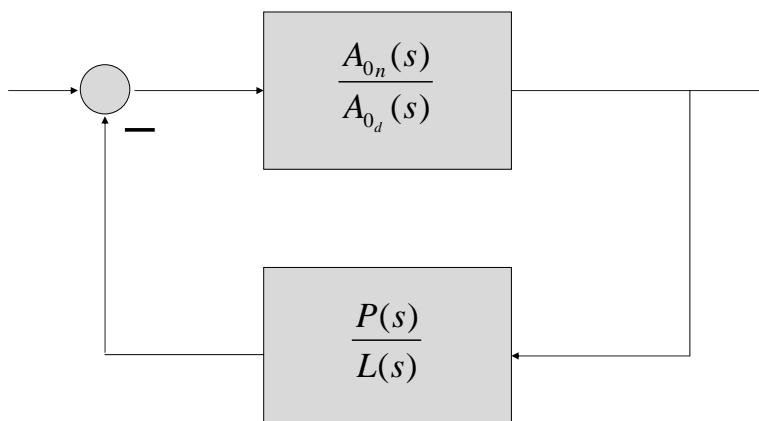


Figure 7. Block diagram of pole placement method.

Incorporating (32) we have

$$\frac{C(s)}{M(s)(1-C(s))} = \frac{C_n(s)M_d(s)}{M_n(s)(C_d(s)-C_n(s))}. \quad (36)$$

Since the low pass filter $C(s)$ has DC gain of 1, the polynomial $C_d(s) - C_n(s)$ has no constant term, which means that the transfer function (36) has at least one pole at the origin. To obtain suitable dynamic compensators which can be decomposed into $M(s)$ and $C(s)$, we need to design a dynamic compensator for the system $\frac{A_0(s)}{s}$. Observing Fig. 8, it can be seen that the two closed-loop systems have the same characteristic equation. Hence we can find $C(s)$ and $M(s)$ from the transfer function $\frac{1}{s} \frac{P(s)}{L(s)}$. Upon selection of the structure of $C(s)$ and $M(s)$, we can write explicitly the transfer function in (36) and obtain the coefficients of s by equating it to $\frac{1}{s} \frac{P(s)}{L(s)}$.

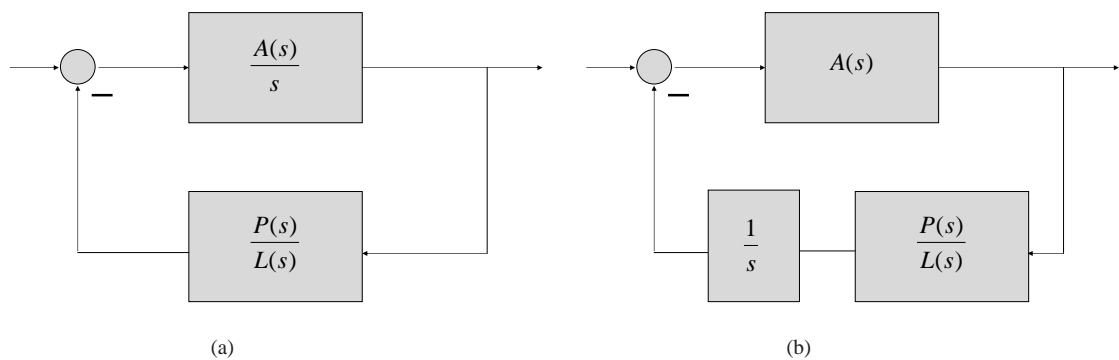


Figure 8. Block Diagrams

Upon obtaining the dynamic compensator $\frac{C(s)}{M(s)(1-C(s))}$, one can apply Nyquist criterion or Root Locus methods to tune the gains of this compensator by changing the poles in $A_{cl}(s)$. If the low-pass filter $C(s)$ and the desired system $M(s)$ do not lead to satisfactory performance, we need to re-select the desired locations of the closed-loop poles. Notice that the above method is an *intuitive one*, and other methods from linear systems theory can be equivalently explored for determining a structure for $C(s)$ and $M(s)$.

We show how to select $M(s)$ and $C(s)$ for our missile model. If we choose the desired pole locations as $-200 \pm 200j$, $-200 \pm 200j$, -20 , -20 and -20 , then

$$A_{cl}(s) = s^7 + 860s^6 + 3.7E05s^5 + 8.4E07s^4 + 1.0E10s^3 + 4.6E11s^2 + 8.2E12s + 5.1E13.$$

The Sylvester Matrix is determined by the coefficients of $A_{0_n}(s)$ and $sA_{0_d}(s)$. The vectors containing the coefficients of $A_{0_n}(s)$ and $sA_{0_d}(s)$, respectively, are shown below

$$[0 \quad -13.5 \quad 16.5 \quad 44796]^\top, \quad [1 \quad 1.06 \quad -290.3 \quad 0 \quad 0]^\top.$$

The Sylvester Matrix S_l is

$$S_l = \begin{bmatrix} 1 & 0 & 0 & 0 & 0 & 0 & 0 & 0 \\ 1.06 & 1 & 0 & 0 & 0 & 0 & 0 & 0 \\ -290.3 & 1.06 & 1 & 0 & -13.5 & 0 & 0 & 0 \\ 0 & -290.3 & 1.06 & 1 & 16.5 & -13.5 & 0 & 0 \\ 0 & 0 & -290.3 & 1.06 & 44796 & 16.5 & -13.5 & 0 \\ 0 & 0 & 0 & -290.3 & 0 & 44796 & 16.5 & -13.5 \\ 0 & 0 & 0 & 0 & 0 & 0 & 44796 & 16.5 \\ 0 & 0 & 0 & 0 & 0 & 0 & 0 & 44796 \end{bmatrix}$$

We solve the following algebraic equation

$$\beta_l = S_l^{-1} \alpha_l$$

to get the vector β_l :

$$\beta_l = [1 \ 858 \ 4.6E06 \ 2.4E08 \ 3.1E05 \ 1.2E07 \ 1.8E08 \ 1.1E09]^\top,$$

where α_l is the vector of the coefficients of $A_{cl}(s)$.

The first four elements of β_l are the coefficients of $L(s)$, and the rest of the elements are the coefficients of $P(s)$.

Hence,

$$L(s) = s^3 + 858s^2 + 4.6E06s + 2.4E08,$$

$$P(s) = 3.1E05s^3 + 1.2E07s^2 + 1.8E08s + 1.1E09.$$

If we select $C(s)$ to be a second order, relative degree 2 transfer function, and $M(s)$ be third order, relative degree 1 transfer function, we can write explicitly the transfer function in (36) and obtain the coefficients of $M(s)$ and $C(s)$ by equating (36) to $\frac{1}{s} \frac{P(s)}{L(s)}$. The transfer functions for $C(s)$ and $M(s)$ take the form:

$$M(s) = \frac{s^2 + 806s + 4.5E06}{s^3 + 39.02s^2 + 585s + 3665}, \quad (37)$$

$$C(s) = \frac{3.1E05}{s^2 + 52.61s + 3.1E05}. \quad (38)$$

This selection of $M(s)$ and $C(s)$ generate satisfactory performance according to simulation results shown in Section VI.

V.A.2. Stability check

We notice that the design of the dynamic compensator is based on our knowledge of the nominal plant $A_0(s)$. We know the bounds for the variation of the system parameters, but not the exact values of these parameters. The stability

of the transfer function (31), or equivalently stability of the condition (20) can be checked by Kharitonov's Theorem. Towards that end, consider the set $\mathcal{I}(s)$ of real polynomials of degree n of the form

$$\delta(s) = \delta_0 + \delta_1 s + \delta_2 s^2 + \delta_3 s^3 + \cdots + \delta_n s^n,$$

where the coefficients lie within the given ranges:

$$\delta_0 \in [X_0, Y_0], \quad \delta_1 \in [X_1, Y_1], \quad \cdots, \quad \delta_n \in [X_n, Y_n].$$

Let $c_\delta = [\delta_0, \delta_1, \cdots, \delta_n]$ and consider the polynomial $\delta(s)$ with its coefficient vector c_δ . Introduce the hyper-rectangle box of the coefficients

$$\mathcal{B} := \{c_\delta : c_\delta \in \mathbb{R}^{n+1}, X_i \leq \delta_i \leq Y_i, i = 0, 1, \cdots, n\}.$$

We assume that the degree remains invariant over the family, so that $0 \notin [X_n, Y_n]$. Kharitonov's Theorem provides a (conservative) necessary and sufficient condition for Hurwitz stability of the entire family.

Theorem 2 (Kharitonov Theorem) [6]

Every polynomial in the family $\mathcal{I}(s)$ is Hurwitz if and only if the following four extreme polynomials are Hurwitz:

$$\begin{aligned} K^1(s) &= X_0 + X_1 s + Y_2 s^2 + Y_3 s^3 + X_4 s^4 + X_5 s^5 + Y_6 s^6 + \cdots, \\ K^2(s) &= X_0 + Y_1 s + Y_2 s^2 + X_3 s^3 + X_4 s^4 + Y_5 s^5 + Y_6 s^6 + \cdots, \\ K^3(s) &= Y_0 + X_1 s + X_2 s^2 + Y_3 s^3 + Y_4 s^4 + X_5 s^5 + X_6 s^6 + \cdots, \\ K^4(s) &= Y_0 + Y_1 s + X_2 s^2 + X_3 s^3 + Y_4 s^4 + Y_5 s^5 + X_6 s^6 + \cdots. \end{aligned}$$

Proof of this theorem is omitted. To show the relationship between the box \mathcal{B} and the vertices corresponding to extreme polynomials, a plot is shown for a family of second order polynomials [7], Fig. 9.

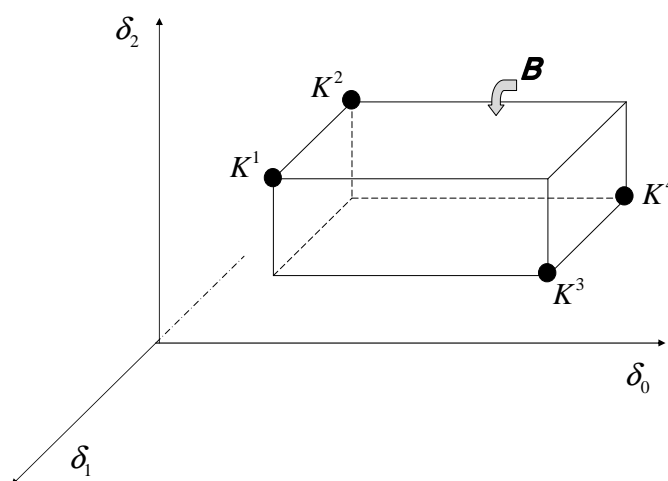


Figure 9. The box \mathcal{B} and four Kharitonov vertices

If we consider the bounds of parametric variations in $A(s)$ in (34) upon designing $C(s)$ and $M(s)$, we can obtain the variation range $[X_i, Y_i]$, $i = 0, 1, \cdots, n$ of each coefficient of the polynomial $H_d(s)$. Substituting X_i and Y_i into

the four extreme polynomials, we only need to check the stability of these four polynomials. If these four polynomials are stable, the designed $C(s)$ and $M(s)$ are acceptable for verification of the condition in (20).

Upon the design of transfer functions $C(s)$ and $M(s)$, the condition (21) needs to be checked. This follows from the same procedure of the results in Cao and Hovakimyan [8, 9].

V.B. Performance

The second step is to ensure satisfactory performance. Upon determining the structure of $M(s)$ and $C(s)$, which can satisfy the sufficient conditions for stability, we can tune the parameters of $M(s)$ and $C(s)$ within the acceptable parameter space to achieve satisfactory performance. The tuning of parameters for $M(s)$ follows from conventional linear systems theory, which we omit here. The guideline for tuning the low-pass filter $C(s)$ follows the same lines of Cao and Hovakimyan [8, 9]. The trade-off between the time-delay margin and the performance of the \mathcal{L}_1 adaptive controller depends solely upon $C(s)$. Increasing the bandwidth of $C(s)$ leads to improved performance at the price of reduced time-delay margin. In [10], we consider constrained optimization of the performance and/or the robustness of \mathcal{L}_1 adaptive controller by resorting to appropriate Linear Matrix Inequality (LMI) type conditions. If the corresponding LMI has a solution, then arbitrary desired performance bound can be achieved, while retaining a prespecified lower-bound on the time-delay margin.

In summary, to gain more freedom in design, it is important for designers to find the largest possible acceptable parameter space in the first step discussed in section V.A.

VI. Simulation Example

The nominal transfer function of the unstable non-minimum phase missile plant in (15) is repeated below:

$$A(s) = \frac{-13.51s^2 + 16.46s + 44800}{s^3 + 1.064s^2 - 290.3s}, \quad (39)$$

and the desired system $M(s)$ and the low-pass filter $C(s)$ are taken from (37) and (38):

$$M(s) = \frac{s^2 + 806s + 4.5E06}{s^3 + 39.02s^2 + 585s + 3665}, \quad (40)$$

$$C(s) = \frac{3.1E05}{s^2 + 52.61s + 3.1E05}. \quad (41)$$

We select $T = 0.0001$. The \mathcal{L}_1 output feedback adaptive control approach is applied to this system. Fig. 10 shows the system outputs with \mathcal{L}_1 controller, in the absence and in the presence of parametric uncertainties. We can see that the system output tracks the step command satisfactorily. Although this response is different from that of the baseline LQR controller, we demonstrate later that in different unknown scenarios, the \mathcal{L}_1 controlled system still has a uniform response close to the one shown in Fig. 10, independent of the nature of the uncertainty. This verifies the theoretical claim on uniform approximation of the corresponding signals of a bounded reference system. In Fig. 11 the control signal is shown, which is guaranteed to stay in low frequency range.

The disturbance is then introduced, as shown in Fig. 12. Since $d(t)$ does not depend on the system output $y(t)$, the condition in (21) is satisfied automatically. We see that the output response is slightly different than that of the nominal \mathcal{L}_1 case, but is still satisfactory. To explain this, we look into the closed loop reference system (19). It can be shown that

$$\begin{aligned} y_{ref}(s) &= M(s) [C(s)r(s) + (1 - C(s))\sigma_{ref}(s)] \\ &= M(s) \left[C(s)r(s) + \frac{C(s)(1 - C(s))(A(s) - M(s))}{M(s) + (A(s) - M(s))C(s)} r(s) + \frac{(1 - C(s))A(s)}{M(s) + (A(s) - M(s))C(s)} d(s) \right]. \end{aligned}$$

The transfer function from $d(s)$ to $y_{ref}(s)$ can be expressed as

$$\frac{(C_d(s) - C_n(s))A_n(s)M_n(s)}{(C_d(s) - C_n(s))A_d(s)M_n(s) + A_n(s)M_d(s)C_n(s)}. \quad (42)$$

The magnitude curve of the Bode diagram is given in Fig. 13, which shows disturbance attenuation at low and high frequencies. This behavior of the reference system can be improved by manipulating the bandwidths of $M(s)$ and $C(s)$. For our non-minimum phase, unstable system $A(s)$, the possible selections are not many.

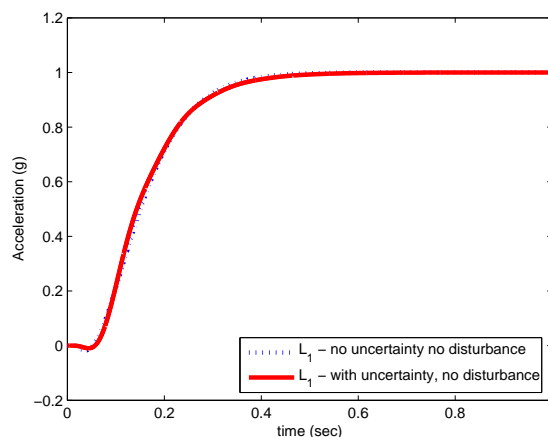


Figure 10. Closed loop response of \mathcal{L}_1 controller - with/without uncertainties, no disturbance

Finally the parametric uncertainties are changed due to a change in aerodynamic coefficients given below:

$$C'_{z\alpha_0} = 1.2 \cdot C_{z\alpha_0}, \quad C'_{m\alpha_0} = 1.5 \cdot C_{m\alpha_0}, \quad C'_{z\delta_{p0}} = 0.8 \cdot C_{z\delta_{p0}}, \quad C'_{m\delta_{p0}} = 0.7 \cdot C_{m\delta_{p0}}. \quad (43)$$

The system output is shown in Fig. 14. We can see that the \mathcal{L}_1 output feedback adaptive control still has uniform performance.

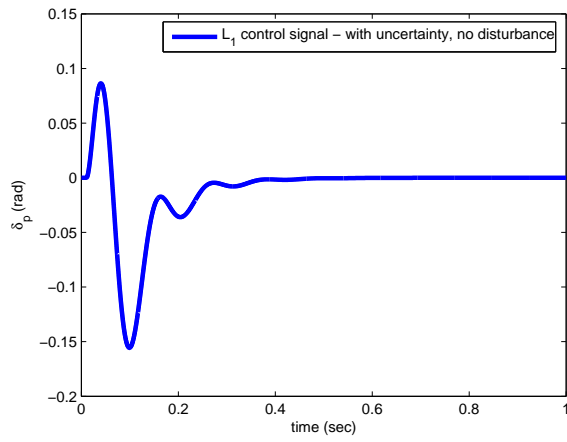


Figure 11. Control signal of \mathcal{L}_1 controller

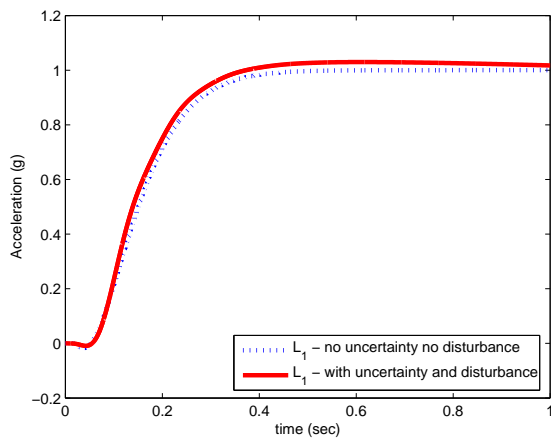


Figure 12. Closed loop response of \mathcal{L}_1 controller - with uncertainties and disturbance

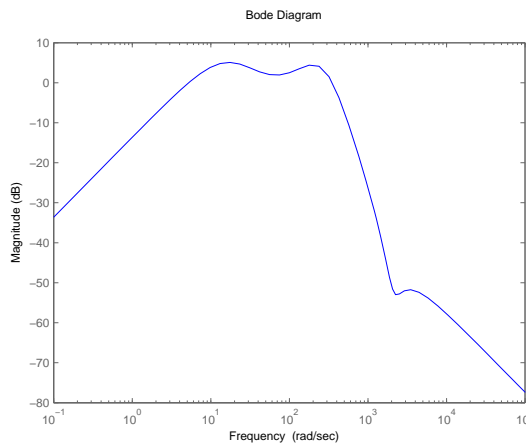


Figure 13. Frequency response of transfer function from d to y_{ref}

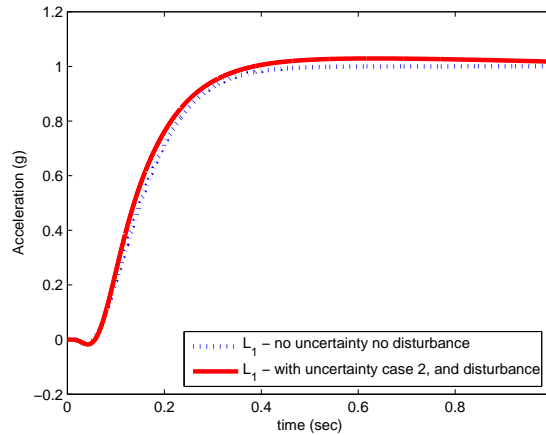


Figure 14. Closed loop response of \mathcal{L}_1 controller with different uncertainties

VII. Conclusion

Longitudinal autopilot design for a missile model is performed using \mathcal{L}_1 adaptive output feedback controller, appropriate for non-SPR reference system dynamics. The new piece-wise constant adaptive law along with the low-pass filtered control signal ensures uniform performance bounds for system's both input/output signals as compared to the corresponding signals of a non-SPR reference system. The simulation responses of the proposed controller are compared to those of baseline LQR and LQG/LTR design, and the benefits of the \mathcal{L}_1 adaptive controller are clearly demonstrated.

VIII. Acknowledgment

This material is based upon work supported by the AFOSR under Contract FA9550-08-1-0135. Any opinions, findings and conclusions or recommendations expressed in this material are those of the authors and do not necessarily reflect the views of United States Air Force.

References

- ¹C. P. Mracek and D. B. Ridgely, Missile Longitudinal Autopilots: Connections Between Optimal Control and Classical Topologies, *Proceedings of AIAA Guidance, Navigation, and Control Conference and Exhibit*, San Francisco, CA, 2005.
- ²C. Cao and N. Hovakimyan, \mathcal{L}_1 Adaptive Output Feedback Controller for Systems of Unknown Relative Degree, *Submitted to American Control Conference*, 2009.
- ³C. Cao and N. Hovakimyan, \mathcal{L}_1 Adaptive Output Feedback Controller for Non Strictly Positive Real Reference Systems, *Submitted to American Control Conference*, 2009.
- ⁴C. Cao and N. Hovakimyan. \mathcal{L}_1 Adaptive Output Feedback Controller for Systems of Unknown Dimension. *IEEE Transactions on Automatic Control*, 53:815–821, April 2008.
- ⁵P. A. Ioannou and J. Sun, *Robust Adaptive Control*. NJ, Prentice Hall, 1995.

⁶V. L. Kharitonov, Asymptotic Stability of an Equilibrium Position of a Family of Systems of Linear Differential Equations, *Differential Uravnen*, 14:2086-2088, 1978.

⁷S. P. Bhattacharyya, H. Chapellat and L. H. Keel, *Robust Control: The Parametric Approach*. NJ, Prentice Hall, 1995.

⁸C. Cao and N. Hovakimyan, Design and Analysis of a Novel \mathcal{L}_1 Adaptive Control Architecture, Part I: Control Signal and Asymptotic Stability, *American Control Conference*, pages 3397-3402, 2006.

⁹C. Cao and N. Hovakimyan, Design and Analysis of a Novel \mathcal{L}_1 Adaptive Control Architecture, Part II: Guaranteed Transient Performance, *American Control Conference*, pages 3403-3408, 2006.

¹⁰D. Li, N. Hovakimyan, C. Cao and K. Wise, Filter Design for Feedback-loop Trade-off of \mathcal{L}_1 Adaptive Controller: A Linear Matrix Inequality Approach, *Proceedings of AIAA Guidance, navigation and Control Conference*, Honolulu, HI, August 2008.